Open database searching enables the identification and comparison of glycoproteomes without defining glycan compositions prior to searching

Ameera Raudah Ahmad Izaham[1] and Nichollas E. Scott[1#]

[1]Department of Microbiology and Immunology, University of Melbourne at the Peter Doherty Institute for Infection and Immunity, Melbourne 3000, Australia

To whom correspondence and requests for materials should be addressed N.E.S (Nichollas.scott@unimelb.edu.au).

Running title: glycopeptide identification independent of glycan databases

ABBREVIATIONS

mass spectrometry (MS)

Luria Bertani (LB)

phosphate-buffered saline (PBS)

sodium dodecyl sulfate (SDS)

normalized collisional energy (NCE)

Zwitterionic Hydrophilic Interaction Liquid Chromatography (ZIC-HILIC)

Trifluoroacetic acid (TFA)

Electron-transfer/higher-energy collision dissociation (EThcD)

higher-energy collision dissociation (HCD)

Collision-induced dissociation (CID)

Automatic Gain Control (AGC)

2,4-diacetamido-2,4,6 trideoxyglucopyranose (diNAcBac)

peptide spectrum matches (PSMs)

Glucose (Glc)

galactose (Gal)

N-Acetylgalactosamine (GalNAc)

N-Acetylglucosamine (GlcNAc)

N-acetylhexoseamine (HexNAc)

Hexose (Hex)

GlcNAc3NAcA4OAc (2,3-diacetamido-2,3-dideoxy-α-D-glucuronic acid)

ABSTRACT

Mass spectrometry has become an indispensable tool for the characterisation of glycosylation across biological systems. Our ability to generate rich fragmentation of glycopeptides has dramatically improved over the last decade yet our informatic approaches still lag behind. While glycoproteomic informatics approaches using glycan databases have attracted considerable attention, database independent approaches have not. This has significantly limited high throughput studies of unusual or atypical glycosylation events such as those observed in bacteria. As such, computational approaches to examine bacterial glycosylation and identify chemically diverse glycans are desperately needed. Here we describe the use of wide-tolerance (up to 2000 Da) open searching as a means to rapidly examine bacterial glycoproteomes. We benchmarked this approach using *N*-linked glycopeptides of *Campylobacter fetus subsp. fetus* as well as *O*-linked glycopeptides of *Acinetobacter baumannii* and *Burkholderia cenocepacia* revealing glycopeptides modified with a range of glycans can be readily identified without defining the glycan masses prior to database searching. Utilising this approach, we demonstrate how wide tolerance searching can be used to compare glycan utilisation across bacterial species by examining the glycoproteomes of eight Burkholderia species (*B. pseudomallei; B. multivorans; B. dolosa; B. humptydooensis; B. ubonensis, B. anthina; B. diffusa; B. pseudomultivorans*). Finally, we demonstrate how open searching enables the identification of low frequency glycoforms based on shared modified peptides sequences. Combined, these results show that open searching is a robust computational approach for the determination of glycan diversity within proteomes.

INTRODUCTION

Protein glycosylation, the addition of carbohydrates to proteins, is a widespread and heterogeneous class of protein modifications [1-3]. Within Eukaryotes, multiple glycosylation systems have been identified [1-3] and up to 20% of the proteome is thought to be subjected to this class of modification [4]. Within Eukaryotes, both *N*-linked and *O*-linked glycosylation systems are known to generate highly heterogeneous glycan structures [2, 3] with this glycan heterogeneity important for the function of glycoproteins [5, 6]. Although the glycan repertoire utilised in Eukaryotic systems is thought to be large, the diversity within any given biological sample is constrained by the limited number of monosaccharides used in Eukaryotic systems [7], as well as the expression of proteins required for the construction of glycans such as glycosyltransferases [8]. Experimentally, these constraints lead to only a limited number of glycans being produced across Eukaryotic samples [9, 10] despite the large number of potential glycan structures [11, 12]. This limited diversity within both Eukaryotic *N*-linked and *O*-linked glycans has enabled the development of glycan databases which have facilitated high throughput glycoproteomic studies [13] using tools such as Byonic [14] and pGlyco [15]. Unfortunately, these databases are not suitable for all glycosylation systems and fail to identify glycopeptides modified with novel or atypical glycans such as those found in bacterial glycosylation systems.

Within bacterial systems, glycosylation is increasingly recognised as a common modification [16-19]. While glycosylation in bacteria was first identified in the 1970s [20], it is only within the last two decades that it has become clear that this class of modifications is ubiquitous across

bacterial genera [16, 18, 21]. Unlike Eukaryotic systems, which utilise a relatively small set of monosaccharides, bacterial glycoproteins are decorated with a diverse range of monosaccharides [22] leading to a staggering array of glycan structures [23-32]. This glycan diversity represents a significant challenge to the field as it makes the identification of novel bacterial glycoproteins a non-trivial analytical undertaking. Yet, through advancements in mass spectrometry (MS) [28, 30, 33, 34], these once obscure modifications are increasingly recognisable and are now known to be essential for bacterial fitness [26, 35-38]. Despite our ability to generate rich bacterial glycopeptide data the field still largely uses manual interrogation to identify and characterise novel glycosylation systems [23-32]. This dependency on manual interrogation is not scalable, time-consuming and prone to human error, especially in the detection of glycoform heterogeneity. This is exemplified in our own experience characterising glycosylation in *Acinetobacter baumannii* where our initial analysis overlooked alternative methylated and deacetylated forms of glucuronic acid [26]. Thus, new approaches are needed to ensure bacterial glycosylation studies can be undertaken in a robust and high-throughput manner.

Wide precursor mass tolerance database searching, also known as 'open' or wildcard searching, is an increasingly popular approach for the detection of protein modifications within proteomic datasets [39-43]. The underlying premise of this approach is that by allowing a wide precursor mass tolerance, modified peptides can be detected by the difference in their observed mass from their expected mass. Importantly, this makes the identification of modifications independent of needing to define the modification in the initial search parameters. This

approach has been utilised to examine chemical modifications such as formylation [44] and miss-alkylation events [45] as well as large modifications such as DNA-peptide crosslinks [43]. Although this approach is effective, it is not without trade-offs being computationally more expensive than traditional searches leading to longer search times [46]. To date, these searches have typically been undertaken using ±500 Da tolerances [39-43] although searches using ±1000Da tolerances have also been reported [43, 46]. Despite the growing application of open database searching in Eukaryotic proteomics, few bacterial studies have utilised this technique. That said, alternative strategies such as dependent peptide searching have been used in bacteria to track misincorporation of amino acids [47] and novel forms of glycosylation such as arginine-rhammnosylation [48].

In this study, we demonstrate that wide mass (up to 2000 Da) open database searching enables the rapid identification of bacterial glycopeptides without the need to assign glycan masses prior to database searching. We benchmark this approach using three previously characterised bacterial glycosylation systems, the *N*-linked glycosylation system of *Campylobacter fetus subsp. fetus* NCTC10842 [25], the *O*-linked glycosylation system of *Acinetobacter baumannii* ATCC17978 [26, 49, 50] and the *O*-linked glycosylation system of *Burkholderia cenocepacia* J2315 [23, 37]. Each of these bacteria have increasingly complex proteomes (ranging from 1600 proteins to nearly 7000) enabling us to assess the performance of open database searching across a range of proteome sizes. We find open database searching readily enabled previously characterised glycoforms and microheterogeneity to be identified across all samples. Applying this approach to representative species of the *Burkholderia genus* [23, 37], we provide the first

snapshot of glycosylation across this genus. Consistent with the conservation of the biosynthetic pathway responsible for the Burkholderia *O*-linked glycans [23] all Burkholderia species examined predominately modify their glycoproteins with two glycan structures of similar composition. Excitingly, we demonstrate that open searching also enables low frequency glycoforms to be detected, highlighting that species-specific glycan structures do exist in Burkholderia. Thus, open database searching provides a new platform to enable the identification of new glycan structures in a high-throughput manner.

EXPERIMENTAL PROCEDURES

Bacterial strains and growth conditions: *C. fetus subsp. fetus NCTC 10842* was grown on Brain-Heart Infusion medium (Hardy Diagnostics) with 5% defibrinated horse blood (Hemostat, Dixon, CA) under microaerobic conditions (10% CO_2, 5% O_2, 85% N_2) at 37 °C as previously reported [25]. *Burkholderia pseudomallei* K96243 was grown as previously reported [51] in Luria Bertani (LB) broth. All other bacterial strains were grown overnight LB agar at 37 °C as previously described [37]. Complete details on the strains, their origins, references and proteome databases used in this study are listed in Table 1.

Table 1. Strain list

Strains	Source (Description, Country, Year)	Reference	Proteome database
C. fetus subsp. fetus NCTC 10842	Brain of sheep fetus, France, 1952	[52]	Uniprot: UP000001035

Acinetobacter baumannii ATCC17978	Fatal meningitis of a 4-month old infant, 1951	[53]	GenBank assembly accession: GCA_001593425.2
Burkholderia pseudomallei K96243	Human clinical specimen, Thailand, 1996	[54]	Uniprot: UP000000605
Burkholderia cenocepacia (LMG 16656 / J2315)	Human clinical specimen, United Kingdom, 1989	[55]	Uniprot: UP000001035
Burkholderia multivorans MSMB2008	Soil isolate, Australia, 2012	[56]	Burkholderia Genome Database [57], Strain number: 3016
Burkholderia dolosa AU0158	Human clinical specimen, USA unknown	[58]	Uniprot database: UP000032886
Burkholderia humptydooensis MSMB43	Water isolate, Australia, unknown	[56, 59]	Burkholderia Genome Database [57], Strain number: 4072
Burkholderia ubonensis MSMB22	Soil isolate, Australia, 2001	[58]	Burkholderia Genome Database [57], Strain number: 3404
Burkholderia anthina MSMB649	Soil isolate, Australia, 2010	[56]	Burkholderia Genome Database [57], Strain number: 2849

Burkholderia diffusa MSMB375	Water isolate, Australia, 2008	[56]	Burkholderia Genome Database [57], Strain number: 2966
Burkholderia pseudomultivorans MSMB2199	Soil isolate, Australia, 2011	[56]	Burkholderia Genome Database [57], Strain number: 3251

153

154 **Generation of bacterial lysates for glycoproteome analysis:** Bacterial strains were grown to
155 confluency on agar plates before being flooded with 5 mL of pre-chilled sterile phosphate-
156 buffered saline (PBS) and bacterial cells collected by scraping. Cells were washed 3 times in PBS
157 to remove media contaminates, collected by centrifugation at 10,000 x *g* at 4˚C and then snap
158 frozen. Frozen whole cell samples were resuspended in 4% SDS, 100mM Tris pH 8.0, 20mM
159 Dithiothreitol and boiled at 95˚C with shaking at 2000rpm for 10 min. Samples were clarified by
160 centrifugation at 17,000 x *g* for 10 min, the supernatants then collected, and protein
161 concentration determined by a bicinchoninic acid assay (Thermo Scientific). 1mg of protein
162 from each sample was acetone precipitated by mixing one volume of sample with 4 volumes of
163 ice-cold acetone. Samples were precipitated overnight at -20˚C and then spun down at 16,000G
164 for 10 min at 0˚C. The precipitated protein pellets were resuspended in 80% ice-cold acetone
165 and precipitated for an additional 4 hours at -20˚C. Samples were centrifuged at 17,000 x *g* for
166 10 min at 0˚C, the supernatant discarded, and excess acetone driven off at 65 ˚C for 5 min.
167 Three biological replicates of each bacterial strain were prepared.

168

Digestion of protein samples: Protein digestion was undertaken as previously described with minor alterations [28]. Briefly, dried protein pellets were resuspended in 6 M urea, 2 M thiourea, 40 mM NH4HCO3 and reduced with 20mM Dithiothreitol then alkylated with 40mM chloroacetamide prior to digestion with Lys-C (1/200 w/w) for 3 hours and trypsin (1/50 w/w) overnight. Digested samples were acidified to a final concentration of 0.5% formic acid and desalted with 50 mg tC18 SEP-PAK (Waters corporation, Milford, USA) according to the manufacturer's instructions. tC18 SEP-PAKs columns were conditioned with 10 bed volumes of Buffer B (80% acetonitrile, 0.1% formic acid), then equilibrated with 10 bed volumes of Buffer A* (0.1% TFA, 2% acetonitrile) before use. Samples were loaded on to equilibrated columns then columns washed with at least 10 bed volumes of Buffer A* before bound peptides were eluted with Buffer B. Eluted peptides were dried by using vacuum centrifugation and stored at -20 ˚C.

ZIC-HILIC enrichment of bacterial glycopeptides: ZIC-HILIC enrichment was performed according to Scott N E *et al*, 2011 with minor modifications [28]. ZIC-HILIC Stage-tips [60] were created by packing 0.5cm of 10 µm ZIC-HILIC resin (Millipore, Massachusetts, United States) into p200 tips containing a frit of C8 Empore™ (Sigma) material. Prior to use, the columns were washed with ultra-pure water, followed by 95% acetonitrile and then equilibrated with 80% acetonitrile and 5% formic acid. Digested proteome samples were resuspended in 80% acetonitrile and 5% formic acid. Samples were adjusted to a concentration of 3 µg/µL (a total of 300 µg of peptide used for each enrichment) then loaded onto equilibrated ZIC-HILIC columns. ZIC-HILIC columns were washed with 20 bed volumes of 80% acetonitrile, 5% formic acid to

remove non-glycosylated peptides and bound peptides eluted with 10 bed volumes of ultra-pure water. Eluted peptides were dried by using vacuum centrifugation and stored at -20 ˚C.

Reverse phase LC-MS: ZIC-HILIC enriched samples were re-suspended in Buffer A* and separated using a two-column chromatography set up composed of a PepMap100 C18 20 mm x 75 µm trap and a PepMap C18 500 mm x 75 µm analytical column (Thermo Fisher Scientific). Samples were concentrated onto the trap column at 5 µL/min for 5 minutes with Buffer A (0.1% formic acid) and then infused into an Orbitrap Fusion™ Lumos™ Tribrid™ Mass Spectrometer (Thermo Fisher Scientific) at 300 nl/minute via the analytical column using a Dionex Ultimate 3000 UPLC (Thermo Fisher Scientific). 185-minute analytical runs were undertaken by altering the buffer composition from 2% buffer B to 28% B over 150 minutes, then from 28% B to 40% B over 10 minutes, then from 40% B to 100% B over 2 minutes. The composition was held at 100% B for 3 minutes, and then dropped to 2% B over 5 minutes before being held at 2% B for another 15 minutes. The Lumos™ Mass Spectrometer was operated in a data-dependent mode automatically switching between the acquisition of a single Orbitrap MS scan (120,000 resolution) every 3 seconds and Orbitrap HCD scans of precursors (NCE 30%, maximum fill time 80 ms, AGC $1*10^5$ with a resolution of 15000). Scans containing the HexNAc oxonium ion m/z 204.087 triggered three additional scans per precursor; a Orbitrap EThcD scan (NCE 15%, maximum fill time 250 ms, AGC $2*10^5$ with a resolution of 30000); a ion trap CID scan (NCE 35%, maximum fill time 40 ms, AGC $5*10^4$) and a stepped collision energy HCD scan (using NCE 32%, 40%, 48% for *N*-linked glycopeptide samples and NCE 28%, 38%, 48% for *O*-linked glycopeptide samples with a maximum fill time of 250 ms, AGC $2*10^5$ with a resolution of

30000). For *B. pseudomallei* K96243 samples, duplicate runs were undertaken as above with the Orbitrap EThcD scans modified to use the extended mass range setting (200 m/z to 3000 m/z) to improve the detection of high mass glycopeptide fragment ions [61].

Data Analysis: Raw data files were batched processed using Byonic v3.5.3 (Protein Metrics Inc. [14]) with the proteome databases denoted within Table 1. Data was searched on a desktop with two 3.00GHz Intel Xeon Gold 6148 processors, a 2TB SDD and 128 GB of RAM using a maximum of 16 cores for a given search. For all searches, a semi-tryptic N-ragged specificity was set and a maximum of two miss cleavage events allowed. Carbamidomethyl was set as a fixed modification of cystine while oxidation of methionine was included as a variable modification. A maximum mass precursor tolerance of 5 ppm was allowed while a mass tolerance of up to 10 ppm was set for HCD fragments and 20 ppm for EThcD fragments. For open searching of *C. fetus fetus* samples (*N*-linked glycosylation), the wildcard parameter was enabled allowing a delta mass between 200 Da and 1600 Da on asparagine residues. For open searching of *O*-linked glycosylation samples, the wildcard parameter was enabled allowing a delta mass between 200 Da and 2000 Da on serine and threonine residues. For focused searches, all parameters listed above remained constant except wildcard searching which was disabled and specific glycoforms as identified from open searches included as variable modifications. To ensure high data quality, separate datasets from the same biological samples were combined using R and only glycopeptides with a Byonic score >300 were used for further analysis. This score cut-off is in line with previous reports highlighting that score thresholds greater than at least 150 are required for robust glycopeptide assignments with Byonic [44, 61].

It should be noted that a score threshold of above 300 resulted in false discovery rates of less than 1% for all combined datasets. Pearson correlation analysis of delta mass profiles was undertaken using Perseus [62]. Data visualization was undertaken using ggplot2 within R with all scripts included in the PRIDE uploaded datasets. All mass spectrometry proteomics data (Raw data files, Byonic searches outputs, R Scripts and output tables) have been deposited into the PRIDE ProteomeXchange Consortium repository [63, 64] with the dataset identifier: PXD018587. Data can be accessed using the **username:** reviewer19225@ebi.ac.uk, **Password:** KNcCmH98

Experimental Design and Statistical Rationale: For each bacterial strain examined three biological replicates were prepared and used for glycopeptide enrichments leading to three LC-MS runs per bacterial strain. Three separate enrichments were prepared and run to ensure an accurate representation of the observable glycoproteome was generated. *B. pseudomallei* K96243 biological replicates were run twice with two different instrument methods to improve the characterisation of the 990 Da glycan. For *C. fetus fetus NCTC 10842* unenriched peptide samples were run with identical methods as those used for glycopeptide analysis to assess the presence of formylated glycans prior to enrichment.

RESULTS

Open database searching allows the identification of bacterial *N*-linked glycopeptides

Although open database searching enables the detection of a variety of modifications, to our knowledge, it has not been applied to bacterial systems or the study of atypical forms of

glycosylation. To enable the identification of glycopeptides with complex glycans, large delta mass windows are needed as even modest glycans (>three monosaccharides) would be larger than the 500 Da window typically used [39-43]. Although the tolerance window of open searching tools can be extended above 500 Da, it has been noted that this leads to increased search times [46]. As bacterial systems possess small proteomes, we reasoned that for these samples the overall searching time may not be prohibitive even when large search windows are used. To assess this, we first examined glycopeptide enrichments of *C. fetus fetus NCTC 10842*. *C. fetus fetus* possesses a small proteome (~1600 proteins [65]) and is known to produce two *N*-linked glycans composed of β-GlcNAc-α1,3-[GlcNAc1,6-]GlcNAc-α1,4-GalNAc-α1,4-GalNAc-α1,3-diNAcBac (1243.507Da) and β-GlcNAc-α1,3-[Glc1,6-]GlcNAc-α1,4-GalNAc-α1,4-GalNAc-α1,4-diNAcBac (1202.481Da) where diNAcBac is the bacterial specific sugar 2,4-diacetamido-2,4,6 trideoxyglucopyranose [25].

To assess the viability of open database searching for glycopeptides, we searched *C. fetus fetus* glycopeptide enrichments allowing a wildcard mass of 200Da to 1600 Da on asparagine. 3hr LC-MS runs were able to be processed by open searching in less than 2hours (Supplementary figure 1A). Examination of the detected modifications by binning the observed delta masses in 0.001Da increments demonstrated a clear cluster of modifications with masses >1000Da (Figure 1A). Within these masses 1242.501Da and 1201.475Da were the most numerous delta masses observed (Figure 1A, Supplementary Table 1) yet these are one Dalton off the expected glycoforms of *C. fetus fetus* [25]. Close examination of the observed delta masses reveals evidence of miss-assignments of the mono-isotopic masses by the appearance of satellite peaks

279 [42, 46] differing by exactly one Dalton (Supplementary Figure 2A). Miss-assignments of the
280 mono-isotopic peaks of large glycopeptides is common place [66] and within Byonic is
281 combated by allowing correction for isotope assignment denoted as the "off-by-x" parameter.
282 Examination of the "off-by-x" masses supports the inappropriate mass correction of the
283 1243/1202 Da glycans to the observed 1242/1201 delta masses (Supplementary Figure 2B).
284 These results support that the 1243/1202 Da glycans are readily detected in *C. fetus fetus*
285 samples using open database searching despite splitting of the delta mass observations across
286 multiple masses due to errors in mono-isotope assignments.
287
288 Surprisingly, our open search also revealed additional glycoforms corresponding to formylated
289 glycans (+27.99Da) as well as a modification corresponding to the loss of a HexNAc (-
290 203.079Da) or Hex (-162.053Da) from the 1243Da or 1202Da glycans respectively (Figure 1B).
291 MS/MS analysis supports these delta masses as unexpected but bona fide glycoforms
292 (Supplementary Figure 3A to J). Formylated glycans have been previously observed [25, 28]
293 during ZIC-HILIC enrichment and are most likely artefacts due to the high concentrations of
294 formic acid [44] used during enrichment. Consistent with glycan formylation being artifactual, it
295 is not observed on C. *fetus fetus* glycopeptides within unenriched samples (Supplementary
296 Figure 4). To assess the accuracy of the glycan masses obtained using open searching, we
297 extracted the mean delta mass of the 1243 and 1202 Da glycans using a density based fitting
298 approach [67] (Figure 1C and D). We find the open search defined mass of the 1243Da and
299 1202Da glycans are both within 5 ppm of the known masses [25] supporting that this approach
300 allows high accuracy determination of large modifications. Finally, we assessed the proteome

coverage of our open database approach to a traditional search using the seven identified glycoforms (1040.423Da, 1068.419Da, 1202.475Da, 1230.469Da, 1243.501Da, 1271.497Da, 1299.492Da,Figure 1B) as a focused database [68]. Interestingly, focused searches outperformed the open database search improving the identification of unique glycopeptides by 35% and glycoproteins by 28% (Figure 1D, Supplementary Table 2). This improvement was also associated with an increase in the mean Byonic score of identified glycopeptides (from 456 to 491, Supplementary figure 5). Combined, these results demonstrate open searching allows the detection of heterogeneous bacterial *N*-linked glycopeptides without the need to define glycans prior to searching.

Open database searching allows the identification of bacterial *O*-linked glycopeptides

To assess open searching's compatibility with bacterial O-linked glycopeptides, we examined glycopeptide enrichments of *A. baumannii ATCC17978*. The *A. baumannii* proteome is twice the size of *C. fetus fetus* (~3600 proteins [69]) with glycosylation of both serine and threonine residues reported to date [49]. Within this system, glycoproteins are modified predominantly with the glycan GlcNAc3NAcA4OAc-4-(β-GlcNAc-6-)-α-Gal-6-β-Glc-3-β-GalNAc where GlcNAc3NAcA4OAc corresponds to the bacterial sugar 2,3-diacetamido-2,3-dideoxy-α-D-glucuronic acid (glycan mass 1030.368 Da [49]). Importantly, this terminal glucuronic acid can also be found in methylated as well as un-acetylated states (corresponding to the glycan masses 1044.383 Da and 988.357 Da respectively [26, 49]). *A. baumannii* glycopeptide enrichments were searched allowing a wildcard mass of 200Da to 2000 Da on serine and threonine residues. The increased complexity of this search, both in terms of the number of

amino acids potentially modified as well as the size of the proteome, resulted in a marked increase in the search times per data files to ~10 hours (Supplementary figure 1B). Within these samples, open searching readily enabled the identification of multiple delta masses of similar sizes to the expected glycans of *A. baumannii ATCC17978* as well as the unexpected glycoforms of 827.281 and 1058.358 Da (Figure 2A, Supplementary Table 3). These novel glycan masses are consistent with formylation (+27.99Da) as well as the loss of HexNAc (-203.079Da) from the 1030Da glycan with MS/MS analysis supporting these assignments (Supplementary Figure 6).

Examination of these masses revealed the most numerous delta masses (1029.362 Da, 987.355 Da and 1043.378 Da) were one Dalton less than the expected *A. baumannii* glycan masses (Figure 2B [26, 49]). As with *C. fetus fetus,* inspection of these assignments reveals the incorrect application of the "off-by-x" parameter leading to the splitting of delta masses across multiple mass assignments separated by one Dalton (Supplementary figure 7). Using the masses 1030.368 Da, 988.357 Da, 1044.383 Da, 827.281 Da and 1058.358 Da, we researched these *A. baumannii* datasets to assess the performance of open searching to a focused search. In contrast to the ~35% increase observed in the coverage of the *C. fetus fetus* glycoproteome, we noted a dramatic improvement in the coverage of the *A. baumannii* glycoproteome with a >240% increase in the number of unique glycopeptides and glycoproteins identified (Figure 2C). To understand this dramatic improvement, we examined the 67 glycopeptides unique to the focused search. Within these glycopeptides we noted a large proportion of PSMs corresponded to glycopeptides modified with multiple glycans (Figure 2D, Supplementary table 4). In fact, >20% (494 out of the total 2282 glycopeptide PSMs) corresponded to glycopeptides with

345 greater than one glycan attached. Within these PSMs, 31 unique peptide sequences are only
346 observed with >1 glycan attached (Figure 2E). Similar to the *N*-linked glycopeptides of *C. fetus*
347 *fetus,* the improvement in the total number of identifications is also associated with an increase
348 in the mean observed Byonic score (from 555 to 601, Supplementary Figure 8). It is important
349 to note that the delta masses of multiply glycosylated peptides fall outside the 2000 Da window
350 used for open searching making the inability to detect these glycopeptides an expected
351 limitation of the search parameters. Thus, although open searching enables the rapid
352 identification of glycopeptides, large glycans / multiply glycosylated peptides can be overlooked
353 supporting the value of a two-step (open followed by focused) searching approach.
354
355 **Open database searching enables the identification of glycosylation within large proteomes**
356 As open searching enabled the identification of both N and O-linked glycopeptides, we sought
357 to explore the compatibility of this approach with larger proteomes using the bacteria B.
358 Cenocepacia J2315 as a model. The *B. Cenocepacia* proteome encodes ~7000 proteins [70] and
359 possesses an *O*-linked glycosylation system responsible for modifying at least 23 proteins [37].
360 Previously, we showed that this glycosylation system transfers two glycans composed of β-Gal-
361 (1,3)-α-GalNAc-(1,3)-β-GalNAc and Suc-β-Gal-(1,3)-α-GalNAc-(1,3)-β-GalNAc where Suc is
362 Succinyl with these glycans corresponding to the masses 568.211Da and 668.228Da
363 respectively [23, 37]. As with *A. baumannii,* the increased complexity of this proteome led to an
364 increase in the search time with individual data files taking ~20hours to process
365 (Supplementary figure 1C). These open searches revealed the presence of the expected
366 glycoforms of *B. cenocepacia* (568.207Da and 668.223Da) as well as additional formylated

variants (596.202Da, 624.197, and 696.218Da) leading to the identification of five unique glycoforms (Figure 3A, Supplementary Table 5). Unlike the large glycans of *C. fetus fetus and A. baumannii,* it is notable that the mono-isotopic mass of the known *B. Cenocepacia* glycans [37] were correctly assigned (Figure 3A). Thus, this supports that for smaller glycans miss-assignment of the mono-isotopic masses during open searches does not appear as problematic.

Incorporating these glycoforms into focused searches again led to a dramatic ~4-fold increase in the number of glycopeptides and a ~2-fold increase in the total number glycoproteins identified compared to open searches (Figure 3B, Supplementary Table 6). Unlike *C. fetus fetus* and *A. baumannii,* this improvement in the total number of identifications was associated with a decrease in the mean Byonic score (from 728 to 700, Supplementary Figure 9). As the dramatic improvement in the glycoproteome coverage of *A. baumannii* was partially driven by the detection of multiply glycosylated peptides we examined the amount of glycosylation within glycopeptide PSMs in *B. Cenocepacia*. As *B. Cenocepacia* glycopeptides modified with multiple glycans would be less than 2000 Da, we were surprised by the limited number of multiply glycosylated peptides identified within our open searches (<10% of all identified glycopeptides, Supplementary figure 10). In contrast, focused searches identified ~40% of all PSMs (Figure 3C, 1508 out of 3937 identified glycopeptide PSMs) corresponded to multiply modified peptides. This data supports that, although open searching performs well for singly modified peptides, this approach appears to underrepresent multiply glycosylated peptides even if the combined mass of the glycan is within the range of the open search.

Open database searching allows the screening of glycan utilisation across biological samples

Having established that open searching enables the identification of a range of glycans, we sought to explore if this could also facilitate the comparison of glycan diversity across bacterial samples. Recently, we reported that a single-loci was responsible for the generation of the O-linked glycans in *B. Cenocepacia* and that this loci is conserved across the *Burkholderia* [23]. Although these results support that Burkholderia species utilise similar glycans, it has been noted that within other bacterial genera extensive glycan heterogeneity exists [25, 26, 29, 32]. As glycan heterogeneity can be challenging to predict, we reasoned that open searching would provide a means to assess the similarities in glycans used across Burkholderia species. We examined glycopeptide enrichments from eight species of Burkholderia (*B. pseudomallei K96243; B. multivorans MSMB2008; B. dolosa AU0158; B. humptydooensis MSMB43; B. ubonensis MSMB22, B. anthina MSMB649; B. diffusa MSMB375; and B. pseudomultivorans MSMB2199*). Examination of the delta masses observed across these eight species demonstrate that the 568Da and 668Da glycoforms as well as their formylated variants are present in all strains (Figure 4A and Supplementary Figure 11, Supplementary Tables 7 to 14). Having generated "delta mass fingerprints" for each species, we assessed if these profiles could enable the comparison across samples using Pearson correlation and hierarchical clustering (Figure 4B and Supplementary Figure 12). Consistent with the similarities in the delta mass fingerprints Pearson correlation and hierarchical clustering resulted in the grouping of all Burkholderia species compared to the delta mass fingerprints of *C. fetus fetus* and *A. baumannii* (Figure 4B). These result support that consistent with the conservation of the glycosylation loci within Burkholderia, the major glycoforms observed within Burkholderia species, based on mass at

411 least, are identical. It should be noted that as with the above glycopeptide datasets, focused
412 searches significantly improved the identification of glycopeptides and glycoproteins in all
413 Burkholderia species (Supplementary figure 13, Supplementary Table 15 to 22).
414
415 **Open database searching allows the detection of glycoforms identified at a low frequency**
416 **based on known glycosylatable peptides**
417 In addition to allowing the comparison of glycan diversity across species, we reasoned that
418 open searching would also allow the identification of novel glycans based on the shared
419 utilization of glycosylatable peptide sequences. Within bacterial glycosylation studies, proteins
420 compatible with different glycosylation machinery are routinely used to "fish" out glycans used
421 for protein glycosylation in different bacterial species [26, 32]. As such, we reasoned the
422 identification of peptides modified with the 568/668Da glycans within Burkholderia species
423 may provide the means to detect alternative glycans used for glycosylation. To assess this, we
424 examined the glycopeptide enrichments of *B. pseudomallei* K96243 filtering for delta masses
425 only observed on peptide sequences also modified with either the 568/668Da glycans (Figure
426 5A). Examination of these delta masses readily revealed the presence of PSMs matching the
427 modification of peptides with single (203.077Da) or double (406.158Da) HexNAc residues, two
428 568Da glycans (1136.422Da) and an unexpected mass at 990.390Da (Figure 5A). Examination of
429 PSMs assigned to this 990Da delta mass revealed a linear glycan composed of HexNAc-Heptose-
430 Heptose-188-215 where the 188 Da and 215 Da are moieties of unknown composition (Figure
431 5B). Incorporation of this unexpected glycan mass into a focused search with the known
432 Burkholderia glycans demonstrate that less than 6% of all glycopeptide PSMs correspond to this

novel glycan (Figure 5C). Thus, this demonstrates that open searching provides an effective means to detect unexpected glycoforms which could be overlooked due to the low frequency of their occurrence in glycoproteomic datasets.

DISCUSSION

MS analysis of glycoproteomic samples typically requires knowledge of both the proteome and possible glycan compositions to facilitate software-based identification [13]. As bacterial glycosylation systems do not utilize glycans found in Eukaryotic glycan databases [23-32], we sought to establish an alternative approach for the high-throughput analysis of bacterial glycoproteomes. Within this work we demonstrate that wide mass open database searching enables the identification of glycosylation without the need to define glycan masses prior to searching. This approach overcomes a significant bottleneck in the identification and characterization of novel bacterial glycosylation systems. We demonstrate that a range of diverse glycan structures, both known [25, 26, 37, 49] as well as not previously reported such as the 990 Da glycan observed in *B. pseudomallei* K96243, can be identified with this approach. In addition, we also demonstrate that open database searches can be used to provide a simple means to compare delta mass profiles across biological samples. This enables a straightforward method to compare and contrast bacterial glycoproteomes, enabling the grouping of Burkholderia profiles from non-similar glycoproteomes such as those seen in *C. fetus fetus* or *A. baumannii*.

Within this work we utilized open searching within Byonic, a widely used tool in the glycoproteomic community for the analysis of glycosylation [61, 71, 72]. This enabled us to directly compare the performance of open searches to focused glycopeptide searches within the same platform. We observed a marked improvement in glycopeptide and glycoprotein identifications within focused searches, especially for glycopeptides modified with multiple glycans. As a number of unique considerations which are not implemented in open searches, such as accounting for oxonium ions and glycan fragments [13, 73], are needed for optimal glycopeptide identification, this improvement in performance is unsurprising. Consistent with this we observe an increase in the mean Byonic score within focused searches compared to open searches for most datasets (Supplementary figure 5, 8 and 9). This improvement translates to an increase in the numbers of unique glycopeptides and glycoproteins identified by ~35% to 240%. This is in line with previous studies which have shown non-optimized settings for glycopeptide analysis can lead to a reduction in glycoproteome coverage [68]. Although Byonic was used within this study it should be noted alternative non-commercial platforms such as MSfragger [43] also allow open searching. In our hands MSfragger performed comparably to Byonic for the identification of glycoforms using open searches (Supplementary Figure 14A to F). Yet as with our open Byonic searches MSfragger did not identify as many unique glycopeptides / glycoproteins as focused Byonic searches (Supplementary Figure 15A to F). These results demonstrate that open searching can be used to identify glycopeptides, yet due to the unique challenges associated with glycopeptide identification open searches can be less sensitive than focused searches.

476 At its core, this analytical approach utilizes a "strength in numbers" based strategy for the
477 detection of glycans. A key strength of this approach is that it does not require the
478 identification of unmodified versions of a peptide for the modified forms to be identified as
479 required in dependent peptide based approaches [47, 48]. This independence of the need for
480 unmodified peptides also makes this approach compatible with enrichment strategies such as
481 ZIC-HILIC glycopeptide enrichment. This is important as for optimal performance this approach
482 requires large numbers of PSMs with identical delta masses. Within this work we focused on
483 bacterial glycosylation systems known to target multiple protein substrates [16, 18], ensuring
484 large numbers of unique PSMs / peptide sequences would be identified. We found that, within
485 glycopeptide enrichments, the known glycoforms of *C. fetus fetus*, *A. baumannii* and *B.*
486 *cenocepacia* were easily detected while infrequently observed glycans, such as the 990Da
487 glycan observed within *B. pseudomallei*, required additional filtering to distinguish this from
488 background signals. This supports that although open searching enables the detection of
489 glycoforms, it is sensitive to the frequency at which modification events are observed within
490 datasets. Although we utilized filtering based on glycosylatable peptide sequences to identify
491 low frequency events, It should be noted that recently Kernel density estimation based fitting /
492 signal detection approaches were shown to effectively address this issue in a more general
493 manner [67]. Thus, open database searching provides multiple approaches to identify
494 modifications even those which are poorly resolved from background.
495
496 Although open searching enabled the identification of glycosylation within all bacterial samples,
497 the analysis of *C. fetus fetus* and *A. baumannii* datasets highlighted the commonality at which

mono-isotopic masses of glycopeptides with large glycans (>1000 Da) are miss-assigned. This problem has been highlighted previously [66] and is not unique to glycopeptides with the mono-isotopic mass of other large biomolecules such as cross-linked peptide shown to be miss-assigned in 50 to 75% of PSMs [74]. This miss-assignment of mono-isotopic masses leads to the splitting of the number of observed PSMs with a specific glycan mass across multiple mass channels. Although we demonstrate that these miss-assigned glycopeptides can be readily identified by examining the "off-by-x" parameter, it should be noted that this splitting dilutes the observable glycopeptides at a specific mass, complicating the analysis of glycoproteomes from open searches. This complication, coupled with the lower sensitivity of glycopeptide identification with open searching compared to focused searches discussed above, supports that open searching is a useful discovery tool yet typically under reports unique glycopeptides and glycoproteins within datasets. The simplest solution to this issue is to use open searching as a means to identify glycans which can then be included as variables within a focused search. As highlighted above, this significantly improved glycoproteome coverage and in our hands provided the flexibility of being able to detect novel glycans yet also ensured optimal identification of glycopeptides. Automated pipelines using multi-step searching have already been demonstrated [42, 46] yet to our knowledge these have not been optimized or implemented for glycopeptide identification. Thus, we recommend a multi-step analysis to enable the identification of atypical glycosylation, using open searching to define glycans which are then incorporated into focused searches.

519 Finally, it should be noted that although not the subject of this manuscript, the
520 glycoproteins/glycopeptides identified in this work are themselves a useful resource for the
521 bacterial glycosylation community. Previous studies on *C. fetus fetus*, *A. baumannii* and *B.*
522 *cenocepacia* identified a total of 26, 26 and 23 unique glycoproteins respectively [25, 26, 37] yet
523 the majority of these studies were undertaken on previous generations of MS instrumentation.
524 Within this work, undertaken on a current generation instrument, we observed a marked
525 improvement in the number of glycoproteins identified with 61 (2.3-fold), 53 (2.0-fold) and 125
526 (5.4-fold) glycoproteins identified in *C. fetus fetus*, *A. baumannii* and *B. cenocepacia*
527 respectively. Similarly, our glycoproteomic analysis of the 8 Burkholderia species highlights that
528 at least 70 proteins are glycosylated within each Burkholderia species. Together, this work
529 highlights that the glycoproteomes of most bacterial species are likely far larger than earlier
530 studies suggested with open searching providing an accessible starting point to probe these
531 systems.
532
533 **ACKNOWLEDGEMENTS**
534 This work was supported by a National Health and Medical Research Council of Australia
535 (NHMRC) project grant awarded to NES (APP1100164). We thank the Melbourne Mass
536 Spectrometry and Proteomics Facility of The Bio21 Molecular Science and Biotechnology
537 Institute for access to MS instrumentation and Byonic. We would like to thank Christine
538 Szymanski and Justin Duma for the kind gift of Campylobacter fetus fetus NCTC 10842 lysates;
539 Mitali Sarkar-Tyson and Nicole Bzdyl for providing the Burkholderia pseudomallei K96243
540 lysates; Deborah Yoder-Himes, Mark Mayo, Bart Currie and Amy Cain for kindly providing

Burkholderia strains for this analysis as well as Chris McDevitt and Saleh Alquethamy for providing A. baumannii ATCC17978. We thank Ben Parker and Nick Williamson for their critical feedback on the manuscript.

DATA AVAILABILITY

All raw data is available through the PRIDE repository, PRIDE accession: PXD018587.

username: reviewer19225@ebi.ac.uk, **Password:** KNcCmH98

REFERENCES:

1. Struwe WB, Robinson CV. Relating glycoprotein structural heterogeneity to function - insights from native mass spectrometry. Curr Opin Struct Biol. 2019;58:241-8. doi: 10.1016/j.sbi.2019.05.019.

2. Brockhausen I, Stanley P. O-GalNAc Glycans. In: rd, Varki A, Cummings RD, Esko JD, Stanley P, Hart GW, et al., editors. Essentials of Glycobiology. Cold Spring Harbor (NY) 2015. p. 113-23.

3. Stanley P, Taniguchi N, Aebi M. N-Glycans. In: rd, Varki A, Cummings RD, Esko JD, Stanley P, Hart GW, et al., editors. Essentials of Glycobiology. Cold Spring Harbor (NY) 2015. p. 99-111.

4. Khoury GA, Baliban RC, Floudas CA. Proteome-wide post-translational modification statistics: frequency analysis and curation of the swiss-prot database. Sci Rep. 2011;1. doi: 10.1038/srep00090.

5. Moremen KW, Tiemeyer M, Nairn AV. Vertebrate protein glycosylation: diversity, synthesis and function. Nat Rev Mol Cell Biol. 2012;13(7):448-62. doi: 10.1038/nrm3383.

6. Xu C, Ng DT. Glycosylation-directed quality control of protein folding. Nat Rev Mol Cell Biol. 2015;16(12):742-52. doi: 10.1038/nrm4073.

564 7. Freeze HH, Hart GW, Schnaar RL. Glycosylation Precursors. In: rd, Varki A, Cummings RD,
565 Esko JD, Stanley P, Hart GW, et al., editors. Essentials of Glycobiology. Cold Spring Harbor (NY)
566 2015. p. 51-63.
567 8. Kawano S, Hashimoto K, Miyama T, Goto S, Kanehisa M. Prediction of glycan structures
568 from gene expression data based on glycosyltransferase reactions. Bioinformatics.
569 2005;21(21):3976-82. doi: 10.1093/bioinformatics/bti666.
570 9. Campbell MP, Royle L, Radcliffe CM, Dwek RA, Rudd PM. GlycoBase and autoGU: tools
571 for HPLC-based glycan analysis. Bioinformatics. 2008;24(9):1214-6. doi:
572 10.1093/bioinformatics/btn090.
573 10. Bohm M, Bohne-Lang A, Frank M, Loss A, Rojas-Macias MA, Lutteke T. Glycosciences.DB:
574 an annotated data collection linking glycomics and proteomics data (2018 update). Nucleic
575 Acids Res. 2019;47(D1):D1195-D201. doi: 10.1093/nar/gky994.
576 11. McDonald AG, Tipton KF, Davey GP. A Knowledge-Based System for Display and
577 Prediction of O-Glycosylation Network Behaviour in Response to Enzyme Knockouts. PLoS
578 Comput Biol. 2016;12(4):e1004844. doi: 10.1371/journal.pcbi.1004844.
579 12. Akune Y, Lin CH, Abrahams JL, Zhang J, Packer NH, Aoki-Kinoshita KF, et al.
580 Comprehensive analysis of the N-glycan biosynthetic pathway using bioinformatics to generate
581 UniCorn: A theoretical N-glycan structure database. Carbohydr Res. 2016;431:56-63. doi:
582 10.1016/j.carres.2016.05.012.
583 13. Hu H, Khatri K, Klein J, Leymarie N, Zaia J. A review of methods for interpretation of
584 glycopeptide tandem mass spectral data. Glycoconj J. 2016;33(3):285-96. doi: 10.1007/s10719-
585 015-9633-3.

586 14. Bern M, Kil YJ, Becker C. Byonic: advanced peptide and protein identification software.
587 Curr Protoc Bioinformatics. 2012; Chapter 13:Unit13 20. doi: 10.1002/0471250953.bi1320s40.
588 15. Liu MQ, Zeng WF, Fang P, Cao WQ, Liu C, Yan GQ, et al. pGlyco 2.0 enables precision N-
589 glycoproteomics with comprehensive quality control and one-step mass spectrometry for intact
590 glycopeptide identification. Nat Commun. 2017;8(1):438. doi: 10.1038/s41467-017-00535-2.
591 16. Nothaft H, Szymanski CM. New discoveries in bacterial N-glycosylation to expand the
592 synthetic biology toolbox. Curr Opin Chem Biol. 2019;53:16-24. doi:
593 10.1016/j.cbpa.2019.05.032.
594 17. Szymanski CM, Wren BW. Protein glycosylation in bacterial mucosal pathogens. Nature
595 reviews Microbiology. 2005;3(3):225-37. doi: 10.1038/nrmicro1100.
596 18. Koomey M. O-linked protein glycosylation in bacteria: snapshots and current
597 perspectives. Curr Opin Struct Biol. 2019;56:198-203. doi: 10.1016/j.sbi.2019.03.020.
598 19. Joshi HJ, Narimatsu Y, Schjoldager KT, Tytgat HLP, Aebi M, Clausen H, et al. SnapShot: O-
599 Glycosylation Pathways across Kingdoms. Cell. 2018;172(3):632- e2. doi:
600 10.1016/j.cell.2018.01.016.
601 20. Schaffer C, Messner P. Emerging facets of prokaryotic glycosylation. FEMS microbiology
602 reviews. 2017;41(1):49-91. doi: 10.1093/femsre/fuw036.
603 21. Macek B, Forchhammer K, Hardouin J, Weber-Ban E, Grangeasse C, Mijakovic I. Protein
604 post-translational modifications in bacteria. Nature reviews Microbiology. 2019;17(11):651-64.
605 doi: 10.1038/s41579-019-0243-0.
606 22. Imperiali B. Bacterial carbohydrate diversity - a Brave New World. Curr Opin Chem Biol.
607 2019;53:1-8. doi: 10.1016/j.cbpa.2019.04.026.

608 23. Fathy Mohamed Y, Scott NE, Molinaro A, Creuzenet C, Ortega X, Lertmemongkolchai G,
609 et al. A general protein O-glycosylation machinery conserved in Burkholderia species improves
610 bacterial fitness and elicits glycan immunogenicity in humans. The Journal of biological
611 chemistry. 2019; 294(36):13248-13268 doi: 10.1074/jbc.RA119.009671.
612 24. Harding CM, Nasr MA, Kinsella RL, Scott NE, Foster LJ, Weber BS, et al. Acinetobacter
613 strains carry two functional oligosaccharyltransferases, one devoted exclusively to type IV pilin,
614 and the other one dedicated to O-glycosylation of multiple proteins. Molecular microbiology.
615 2015;96(5):1023-41. doi: 10.1111/mmi.12986.
616 25. Nothaft H, Scott NE, Vinogradov E, Liu X, Hu R, Beadle B, et al. Diversity in the protein N-
617 glycosylation pathways within the Campylobacter genus. Molecular & cellular proteomics :
618 MCP. 2012;11(11):1203-19. doi: 10.1074/mcp.M112.021519.
619 26. Scott NE, Kinsella RL, Edwards AV, Larsen MR, Dutta S, Saba J, et al. Diversity within the
620 O-linked protein glycosylation systems of acinetobacter species. Molecular & cellular
621 proteomics : MCP. 2014;13(9):2354-70. doi: 10.1074/mcp.M114.038315.
622 27. Scott NE, Nothaft H, Edwards AV, Labbate M, Djordjevic SP, Larsen MR, et al.
623 Modification of the Campylobacter jejuni N-linked glycan by EptC protein-mediated addition of
624 phosphoethanolamine. The Journal of biological chemistry. 2012;287(35):29384-96. doi:
625 10.1074/jbc.M112.380212.
626 28. Scott NE, Parker BL, Connolly AM, Paulech J, Edwards AV, Crossett B, et al. Simultaneous
627 glycan-peptide characterization using hydrophilic interaction chromatography and parallel
628 fragmentation by CID, higher energy collisional dissociation, and electron transfer dissociation

MS applied to the N-linked glycoproteome of Campylobacter jejuni. Molecular & cellular proteomics : MCP. 2011;10(2):M000031-MCP201. doi: 10.1074/mcp.M000031-MCP201.

29. Hadjineophytou C, Anonsen JH, Wang N, Ma KC, Viburiene R, Vik A, et al. Genetic determinants of genus-Level glycan diversity in a bacterial protein glycosylation system. PLoS Genet. 2019;15(12):e1008532. doi: 10.1371/journal.pgen.1008532.

30. Ulasi GN, Creese AJ, Hui SX, Penn CW, Cooper HJ. Comprehensive mapping of O-glycosylation in flagellin from Campylobacter jejuni 11168: A multienzyme differential ion mobility mass spectrometry approach. Proteomics. 2015;15(16):2733-45. doi: 10.1002/pmic.201400533.

31. Jervis AJ, Wood AG, Cain JA, Butler JA, Frost H, Lord E, et al. Functional analysis of the Helicobacter pullorum N-linked protein glycosylation system. Glycobiology. 2018;28(4):233-44. doi: 10.1093/glycob/cwx110.

32. Jervis AJ, Butler JA, Lawson AJ, Langdon R, Wren BW, Linton D. Characterization of the structurally diverse N-linked glycans of Campylobacter species. Journal of bacteriology. 2012;194(9):2355-62. doi: 10.1128/JB.00042-12.

33. Madsen JA, Ko BJ, Xu H, Iwashkiw JA, Robotham SA, Shaw JB, et al. Concurrent automated sequencing of the glycan and peptide portions of O-linked glycopeptide anions by ultraviolet photodissociation mass spectrometry. Anal Chem. 2013;85(19):9253-61. doi: 10.1021/ac4021177.

34. Zampronio CG, Blackwell G, Penn CW, Cooper HJ. Novel glycosylation sites localized in Campylobacter jejuni flagellin FlaA by liquid chromatography electron capture dissociation

650 tandem mass spectrometry. Journal of proteome research. 2011;10(3):1238-45. doi:
651 10.1021/pr101021c.
652 35. Cain JA, Dale AL, Niewold P, Klare WP, Man L, White MY, et al. Proteomics reveals
653 multiple phenotypes associated with N-linked glycosylation in Campylobacter jejuni. Molecular
654 & cellular proteomics : MCP. 2019 18(4):715-734. doi: 10.1074/mcp.RA118.001199.
655 36. Elhenawy W, Scott NE, Tondo ML, Orellano EG, Foster LJ, Feldman MF. Protein O-linked
656 glycosylation in the plant pathogen Ralstonia solanacearum. Glycobiology. 2016;26(3):301-11.
657 doi: 10.1093/glycob/cwv098.
658 37. Lithgow KV, Scott NE, Iwashkiw JA, Thomson EL, Foster LJ, Feldman MF, et al. A general
659 protein O-glycosylation system within the Burkholderia cepacia complex is involved in motility
660 and virulence. Molecular microbiology. 2014;92(1):116-37. doi: 10.1111/mmi.12540.
661 38. Abouelhadid S, North SJ, Hitchen P, Vohra P, Chintoan-Uta C, Stevens M, et al.
662 Quantitative Analyses Reveal Novel Roles for N-Glycosylation in a Major Enteric Bacterial
663 Pathogen. MBio. 2019;10(2). doi: 10.1128/mBio.00297-19.
664 39. Chick JM, Kolippakkam D, Nusinow DP, Zhai B, Rad R, Huttlin EL, et al. A mass-tolerant
665 database search identifies a large proportion of unassigned spectra in shotgun proteomics as
666 modified peptides. Nat Biotechnol. 2015;33(7):743-9. doi: 10.1038/nbt.3267.
667 40. Na S, Bandeira N, Paek E. Fast multi-blind modification search through tandem mass
668 spectrometry. Molecular & cellular proteomics : MCP. 2012;11(4):M111 010199. doi:
669 10.1074/mcp.M111.010199.

670 41. Devabhaktuni A, Lin S, Zhang L, Swaminathan K, Gonzalez CG, Olsson N, et al. TagGraph
671 reveals vast protein modification landscapes from large tandem mass spectrometry datasets.
672 Nat Biotechnol. 2019;37(4):469-79. doi: 10.1038/s41587-019-0067-5.
673 42. Solntsev SK, Shortreed MR, Frey BL, Smith LM. Enhanced Global Post-translational
674 Modification Discovery with MetaMorpheus. Journal of proteome research. 2018;17(5):1844-
675 51. doi: 10.1021/acs.jproteome.7b00873.
676 43. Kong AT, Leprevost FV, Avtonomov DM, Mellacheruvu D, Nesvizhskii AI. MSFragger:
677 ultrafast and comprehensive peptide identification in mass spectrometry-based proteomics.
678 Nature methods. 2017;14(5):513-20. doi: 10.1038/nmeth.4256.
679 44. Lenco J, Khalikova MA, Svec F. Dissolving Peptides in 0.1% Formic Acid Brings Risk of
680 Artificial Formylation. Journal of proteome research. 2020;19(3):993-9. doi:
681 10.1021/acs.jproteome.9b00823.
682 45. Muller T, Winter D. Systematic Evaluation of Protein Reduction and Alkylation Reveals
683 Massive Unspecific Side Effects by Iodine-containing Reagents. Molecular & cellular proteomics
684 : MCP. 2017;16(7):1173-87. doi: 10.1074/mcp.M116.064048.
685 46. Li Q, Shortreed MR, Wenger CD, Frey BL, Schaffer LV, Scalf M, et al. Global Post-
686 Translational Modification Discovery. Journal of proteome research. 2017;16(4):1383-90. doi:
687 10.1021/acs.jproteome.6b00034.
688 47. Cvetesic N, Semanjski M, Soufi B, Krug K, Gruic-Sovulj I, Macek B. Proteome-wide
689 measurement of non-canonical bacterial mistranslation by quantitative mass spectrometry of
690 protein modifications. Sci Rep. 2016;6:28631. doi: 10.1038/srep28631.

691 48. Lassak J, Keilhauer EC, Furst M, Wuichet K, Godeke J, Starosta AL, et al. Arginine-
692 rhamnosylation as new strategy to activate translation elongation factor P. Nat Chem Biol.
693 2015;11(4):266-70. doi: 10.1038/nchembio.1751.
694 49. Iwashkiw JA, Seper A, Weber BS, Scott NE, Vinogradov E, Stratilo C, et al. Identification
695 of a general O-linked protein glycosylation system in Acinetobacter baumannii and its role in
696 virulence and biofilm formation. PLoS pathogens. 2012;8(6):e1002758. doi:
697 10.1371/journal.ppat.1002758.
698 50. Lees-Miller RG, Iwashkiw JA, Scott NE, Seper A, Vinogradov E, Schild S, et al. A common
699 pathway for O-linked protein-glycosylation and synthesis of capsule in Acinetobacter
700 baumannii. Molecular microbiology. 2013;89(5):816-30. doi: 10.1111/mmi.12300.
701 51. Bzdyl NM, Scott NE, Norville IH, Scott AE, Atkins T, Pang S, et al. Peptidyl-Prolyl
702 Isomerase ppiB Is Essential for Proteome Homeostasis and Virulence in Burkholderia
703 pseudomallei. Infection and immunity. 2019;87(10). doi: 10.1128/IAI.00528-19.
704 52. VÉRON MC, R. Taxonomic Study of the Genus Campylobacter Sebald and Véron and
705 Designation of the Neotype Strain for the Type Species, Campylobacter fetus (Smith and Taylor)
706 Sebald and Véro. INTERNATIONAL JOURNAL OF SYSTEMATIC BACTERIOLOGY. 1973;23(3):122-
707 34.
708 53. Baumann P, Doudoroff M, Stanier RY. A study of the Moraxella group. II. Oxidative-
709 negative species (genus Acinetobacter). Journal of bacteriology. 1968;95(5):1520-41.
710 54. Holden MT, Titball RW, Peacock SJ, Cerdeno-Tarraga AM, Atkins T, Crossman LC, et al.
711 Genomic plasticity of the causative agent of melioidosis, Burkholderia pseudomallei.

712 Proceedings of the National Academy of Sciences of the United States of America.
713 2004;101(39):14240-5. doi: 10.1073/pnas.0403302101.
714 55. Vandamme P, Holmes B, Vancanneyt M, Coenye T, Hoste B, Coopman R, et al.
715 Occurrence of multiple genomovars of Burkholderia cepacia in cystic fibrosis patients and
716 proposal of Burkholderia multivorans sp. nov. Int J Syst Bacteriol. 1997;47(4):1188-200. doi:
717 10.1099/00207713-47-4-1188.
718 56. Sahl JW, Vazquez AJ, Hall CM, Busch JD, Tuanyok A, Mayo M, et al. The Effects of Signal
719 Erosion and Core Genome Reduction on the Identification of Diagnostic Markers. mBio.
720 2016;7(5). doi: 10.1128/mBio.00846-16.
721 57. Winsor GL, Khaira B, Van Rossum T, Lo R, Whiteside MD, Brinkman FS. The Burkholderia
722 Genome Database: facilitating flexible queries and comparative analyses. Bioinformatics.
723 2008;24(23):2803-4. doi: 10.1093/bioinformatics/btn524.
724 58. Johnson SL, Bishop-Lilly KA, Ladner JT, Daligault HE, Davenport KW, Jaissle J, et al.
725 Complete genome sequences for 59 burkholderia isolates, both pathogenic and near neighbor.
726 Genome Announc. 2015;3(2). doi: 10.1128/genomeA.00159-15.
727 59. Ginther JL, Mayo M, Warrington SD, Kaestli M, Mullins T, Wagner DM, et al.
728 Identification of Burkholderia pseudomallei Near-Neighbor Species in the Northern Territory of
729 Australia. PLoS Negl Trop Dis. 2015;9(6):e0003892. doi: 10.1371/journal.pntd.0003892.
730 60. Rappsilber J, Mann M, Ishihama Y. Protocol for micro-purification, enrichment, pre-
731 fractionation and storage of peptides for proteomics using StageTips. Nature protocols.
732 2007;2(8):1896-906. doi: 10.1038/nprot.2007.261.

733 61. Lee LY, Moh ES, Parker BL, Bern M, Packer NH, Thaysen-Andersen M. Toward
734 Automated N-Glycopeptide Identification in Glycoproteomics. Journal of proteome research.
735 2016;15(10):3904-15. doi: 10.1021/acs.jproteome.6b00438.
736 62. Tyanova S, Temu T, Sinitcyn P, Carlson A, Hein MY, Geiger T, et al. The Perseus
737 computational platform for comprehensive analysis of (prote)omics data. Nature methods.
738 2016;13(9):731-40. doi: 10.1038/nmeth.3901.
739 63. Perez-Riverol Y, Csordas A, Bai J, Bernal-Llinares M, Hewapathirana S, Kundu DJ, et al.
740 The PRIDE database and related tools and resources in 2019: improving support for
741 quantification data. Nucleic Acids Res. 2019;47(D1):D442-D50. doi: 10.1093/nar/gky1106.
742 64. Vizcaino JA, Csordas A, del-Toro N, Dianes JA, Griss J, Lavidas I, et al. 2016 update of the
743 PRIDE database and its related tools. Nucleic Acids Res. 2016;44(D1):D447-56. doi:
744 10.1093/nar/gkv1145.
745 65. Oliveira LM, Resende DM, Dorneles EM, Horacio EC, Alves FL, Goncalves LO, et al.
746 Complete Genome Sequence of Type Strain Campylobacter fetus subsp. fetus ATCC 27374.
747 Genome Announc. 2016;4(6). doi: 10.1128/genomeA.01344-16.
748 66. Shin B, Jung HJ, Hyung SW, Kim H, Lee D, Lee C, et al. Postexperiment monoisotopic
749 mass filtering and refinement (PE-MMR) of tandem mass spectrometric data increases accuracy
750 of peptide identification in LC/MS/MS. Molecular & cellular proteomics : MCP. 2008;7(6):1124-
751 34. doi: 10.1074/mcp.M700419-MCP200.
752 67. Avtonomov DM, Kong A, Nesvizhskii AI. DeltaMass: Automated Detection and
753 Visualization of Mass Shifts in Proteomic Open-Search Results. Journal of proteome research.
754 2019;18(2):715-20. doi: 10.1021/acs.jproteome.8b00728.

755 68. Khatri K, Klein JA, Zaia J. Use of an informed search space maximizes confidence of site-
756 specific assignment of glycoprotein glycosylation. Anal Bioanal Chem. 2017;409(2):607-18. doi:
757 10.1007/s00216-016-9970-5.
758 69. Smith MG, Gianoulis TA, Pukatzki S, Mekalanos JJ, Ornston LN, Gerstein M, et al. New
759 insights into Acinetobacter baumannii pathogenesis revealed by high-density pyrosequencing
760 and transposon mutagenesis. Genes Dev. 2007;21(5):601-14. doi: 10.1101/gad.1510307.
761 70. Holden MT, Seth-Smith HM, Crossman LC, Sebaihia M, Bentley SD, Cerdeno-Tarraga AM,
762 et al. The genome of Burkholderia cenocepacia J2315, an epidemic pathogen of cystic fibrosis
763 patients. Journal of bacteriology. 2009;191(1):261-77. doi: 10.1128/JB.01230-08.
764 71. Parker BL, Thaysen-Andersen M, Solis N, Scott NE, Larsen MR, Graham ME, et al. Site-
765 specific glycan-peptide analysis for determination of N-glycoproteome heterogeneity. Journal
766 of proteome research. 2013;12(12):5791-800. doi: 10.1021/pr400783j.
767 72. Riley NM, Hebert AS, Westphall MS, Coon JJ. Capturing site-specific heterogeneity with
768 large-scale N-glycoproteome analysis. Nat Commun. 2019;10(1):1311. doi: 10.1038/s41467-
769 019-09222-w.
770 73. Darula Z, Medzihradszky KF. Analysis of Mammalian O-Glycopeptides-We Have Made a
771 Good Start, but There is a Long Way to Go. Molecular & cellular proteomics : MCP.
772 2018;17(1):2-17. doi: 10.1074/mcp.MR117.000126.
773 74. Lenz S, Giese SH, Fischer L, Rappsilber J. In-Search Assignment of Monoisotopic Peaks
774 Improves the Identification of Cross-Linked Peptides. Journal of proteome research.
775 2018;17(11):3923-31. doi: 10.1021/acs.jproteome.8b00600.
776

FIGURE LEGENDS

Figure 1: Open searching analysis of C. fetus fetus NCTC 10842 glycopeptides. A) *C. fetus fetus* glycopeptide delta mass plot of 0.001 Dalton increments showing the detection of PSMs modified with masses over 1000 Da. **B)** Zoomed view of *C. fetus fetus* glycopeptide delta mass plot highlighting the most numerous observed delta masses; red masses correspond to non-formylated glycans while black masses correspond to formylated glycans. **C)** Density and zoomed delta mass plot of the *C. fetus fetus* glycan masses 1243.507Da and 1202.481Da. **D)** Comparison of the glycoproteome coverage observed between open and focused searches across *C. fetus fetus* datasets.

Figure 2: Open searching analysis of *A. baumannii ATCC17978* glycopeptides. A) *A. baumannii* glycopeptide delta mass plot of 0.001 Dalton increments showing the detection of PSMs modified with masses over 800 Da. **B)** Zoomed view of *A. baumannii* glycopeptide delta mass plot highlighting the most numerous observed modifications. **C)** Comparison of the glycoproteome coverage observed between open and focused searches across of *A. baumannii* datasets **D)** Glycan mass plot showing the amount of glycan (in Da) observed on glycopeptides PSMs within the focused searches. **E)** Venn diagram showing the number of unique peptide sequences grouped based on the number of glycans observed on these peptides.

Figure 3: Open searching analysis of *B. Cenocepacia* J2315 glycopeptides. A) *B. Cenocepacia* glycopeptide delta mass plot of 0.001 Dalton increments showing the detection of PSMs modified with masses over 500 Da. Highlighted area shown in zoomed panel. **B)** Comparison of

the glycoproteome coverage observed between open and focused searches across *B. Cenocepacia* datasets **C)** Glycan mass plot showing the amount of glycan (in Da) observed on glycopeptides PSMs within the focused searches. Nearly 40% of all glycopeptide PSMs are decorated with two or more glycans.

Figure 4: Comparison of Burkholderia glycoproteomes using open searching. A) Representative delta mass plots of four out of the eight Burkholderia strains examined demonstrating the 568Da and 668Da glycans are frequently identified delta masses in Burkholderia glycopeptide enrichments. Formylated glycans are denotated in black while Burkholderia O-linked glycans are in red. **B)** Pearson correlation and clustering analysis of delta mass plots enable the comparison and grouping of samples.

Figure 5: Identification of minor glycoforms within B. pseudomallei K96243. A) Delta mass plot, binned by 0.001 Dalton increments, showing delta masses observed for peptide sequences also modified with the 568 or 668D glycans. **B)** MS/MS analysis (FTMS-HCD, ITMS-CID and FTMS-EThcD) supporting the assignment of a linear glycan of HexNAc-Heptose-Heptose-188-215 attached to the peptide KAATAAPADAASQ. **C)** Glycan mass plot showing the amount of glycan (in Da) observed on glycopeptides PSMs within focused searches. Only ~6% of all PSMs observed are modified with the 990 Da glycan.

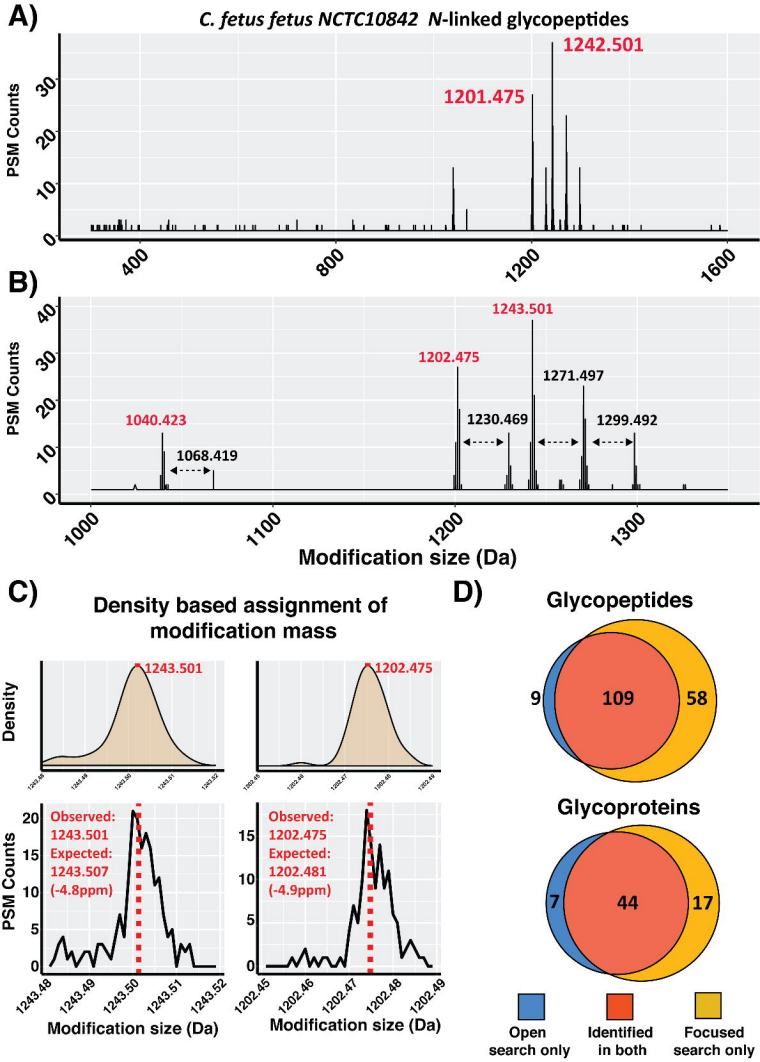
A)
C. fetus fetus NCTC10842 N-linked glycopeptides
PSM Counts
1242.501
1201.475
B)
PSM Counts
1243.501
1202.475
1271.497
1040.423
1230.469
1299.492
1068.419
Modification size (Da)
C)
Density based assignment of modification mass
Density
1243.501
1202.475
PSM Counts
Observed: 1243.501
Expected: 1243.507
(-4.8ppm)
Observed: 1202.475
Expected: 1202.481
(-4.9ppm)
Modification size (Da)
Modification size (Da)
D)
Glycopeptides
9
109
58
Glycoproteins
7
44
17
Open search only
Identified in both
Focused search only

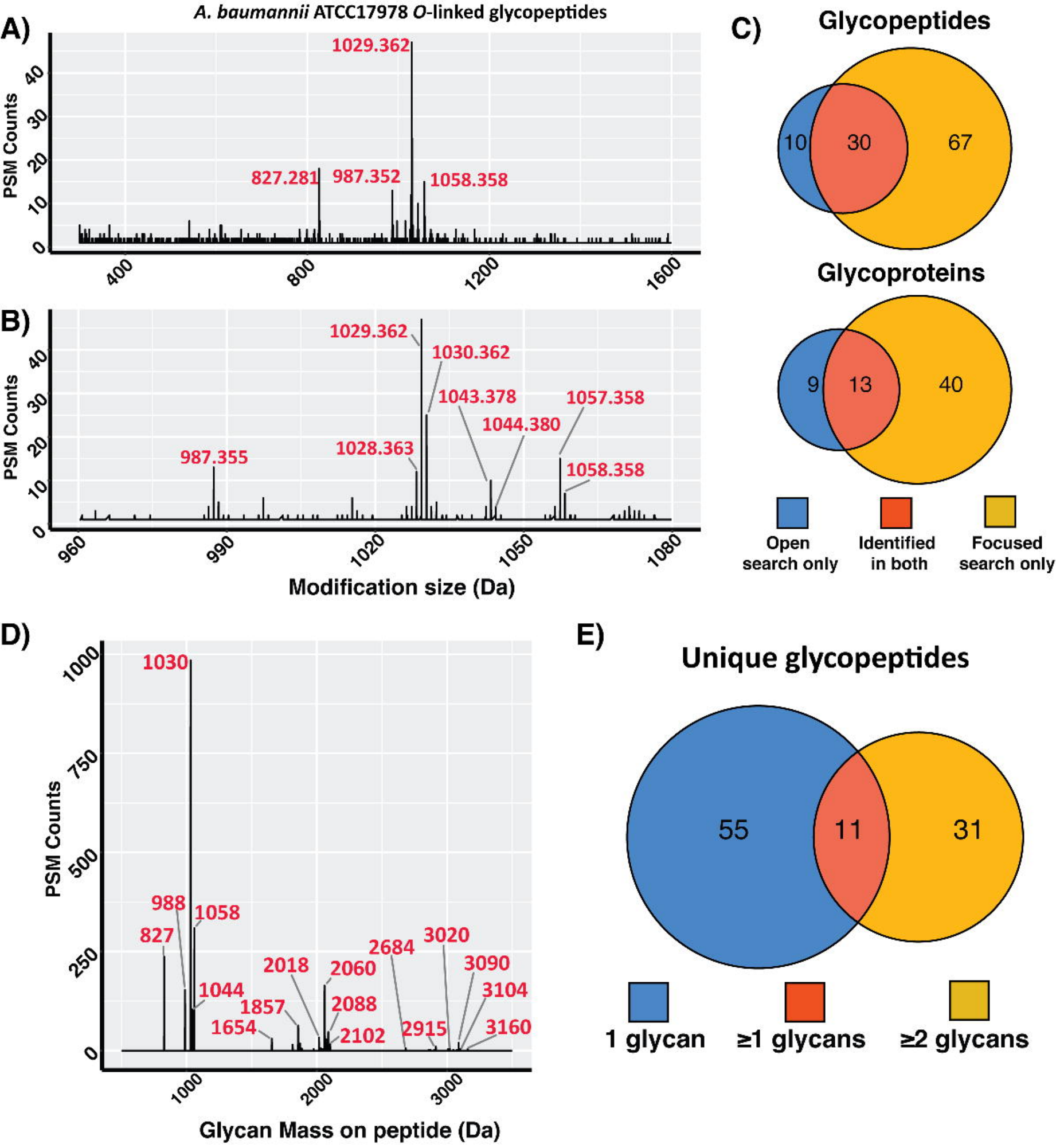
A)
A. baumannii ATCC17978 O-linked glycopeptides
PSM Counts
1029.362
827.281
987.352
1058.358
B)
1029.362
1030.362
1043.378
1057.358
1044.380
1028.363
987.355
1058.358
Modification size (Da)
C)
Glycopeptides
10
30
67
Glycoproteins
9
13
40
Open search only
Identified in both
Focused search only
D)
1030
988
1058
827
1044
1857
1654
2018
2060
2088
2102
2684
2915
3020
3090
3104
3160
Glycan Mass on peptide (Da)
E)
Unique glycopeptides
55
11
31
1 glycan
≥1 glycans
≥2 glycans

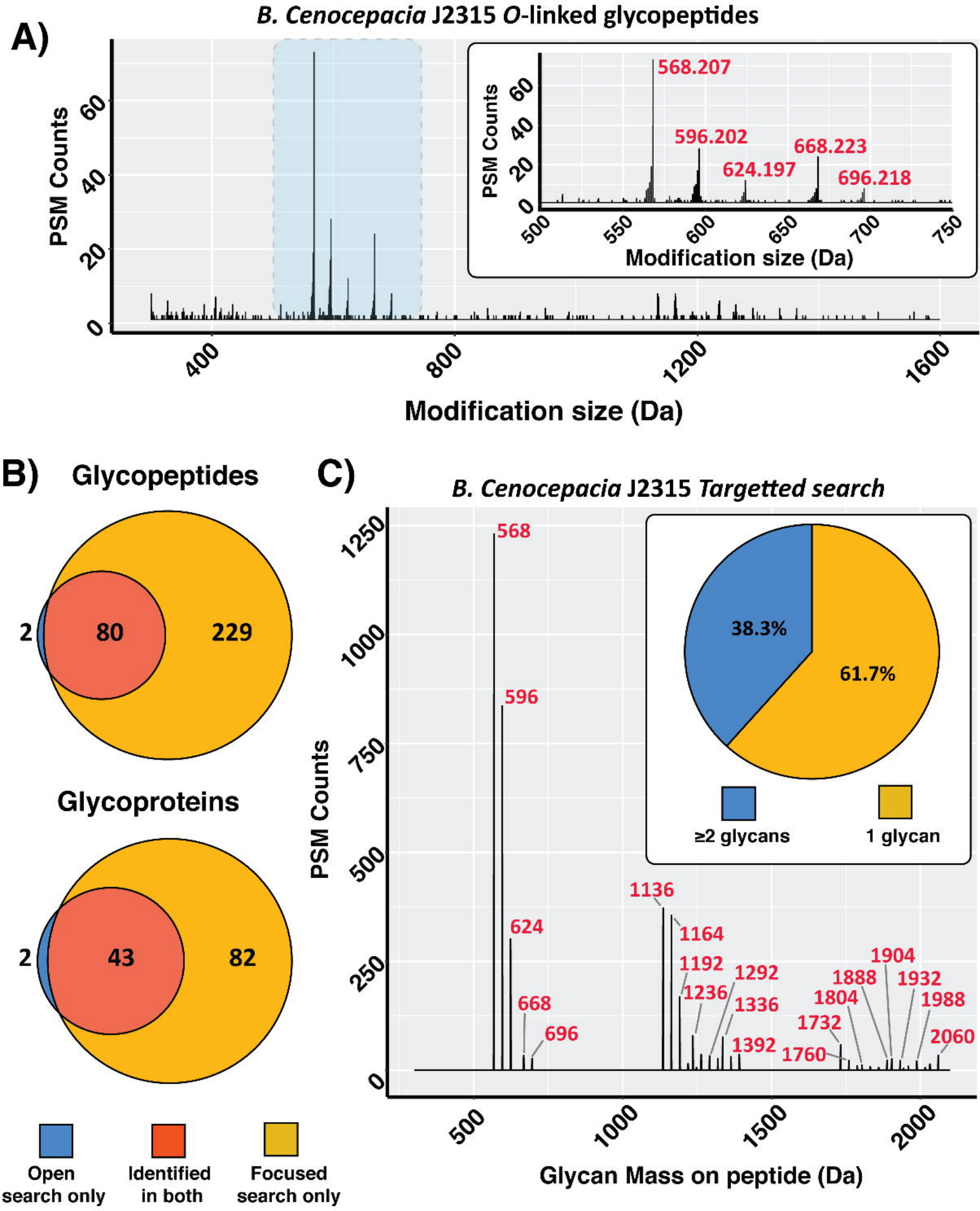
A)
B. Cenocepacia J2315 O-linked glycopeptides
PSM Counts
Modification size (Da)
568.207
596.202
624.197
668.223
696.218
B)
Glycopeptides
2
80
229
Glycoproteins
2
43
82
Open search only
Identified in both
Focused search only
C)
B. Cenocepacia J2315 Targetted search
PSM Counts
Glycan Mass on peptide (Da)
568
596
624
668
696
1136
1164
1192
1236
1292
1336
1392
1732
1760
1804
1888
1904
1932
1988
2060
38.3%
61.7%
≥2 glycans
1 glycan

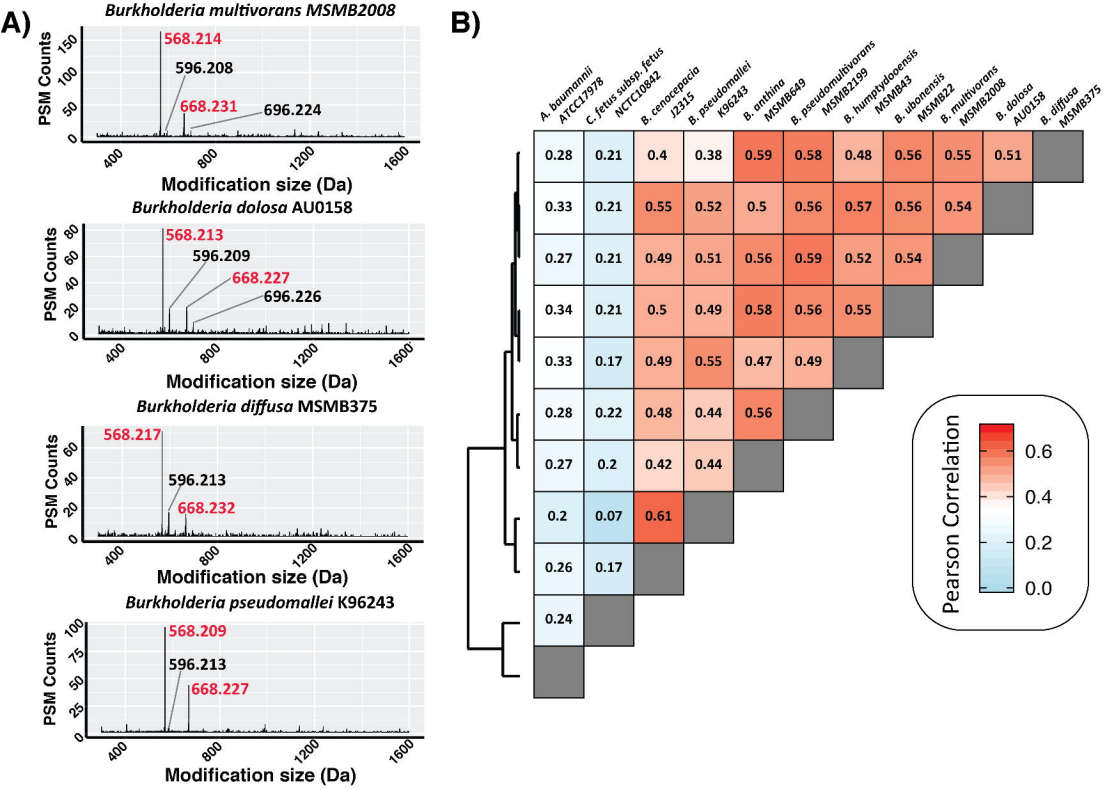
A)
Burkholderia multivorans MSMB2008
PSM Counts
568.214
596.208
668.231
696.224
Modification size (Da)
Burkholderia dolosa AU0158
568.213
596.209
668.227
696.226
Burkholderia diffusa MSMB375
568.217
596.213
668.232
Burkholderia pseudomallei K96243
568.209
596.213
668.227
B)
A. baumannii ATCC17978
C. fetus subsp. fetus NCTC10842
B. cenocepacia J2315
B. pseudomallei K96243
B. anthina MSMB649
B. pseudomultivorans MSMB2199
B. humptydooensis MSMB43
B. ubonensis MSMB22
B. multivorans MSMB2008
B. dolosa AU0158
B. diffusa MSMB375
0.28 0.21 0.4 0.38 0.59 0.58 0.48 0.56 0.55 0.51
0.33 0.21 0.55 0.52 0.5 0.56 0.57 0.56 0.54
0.27 0.21 0.49 0.51 0.56 0.59 0.52 0.54
0.34 0.21 0.5 0.49 0.58 0.56 0.55
0.33 0.17 0.49 0.55 0.47 0.49
0.28 0.22 0.48 0.44 0.56
0.27 0.2 0.42 0.44
0.2 0.07 0.61
0.26 0.17
0.24
Pearson Correlation
0.6
0.4
0.2
0.0

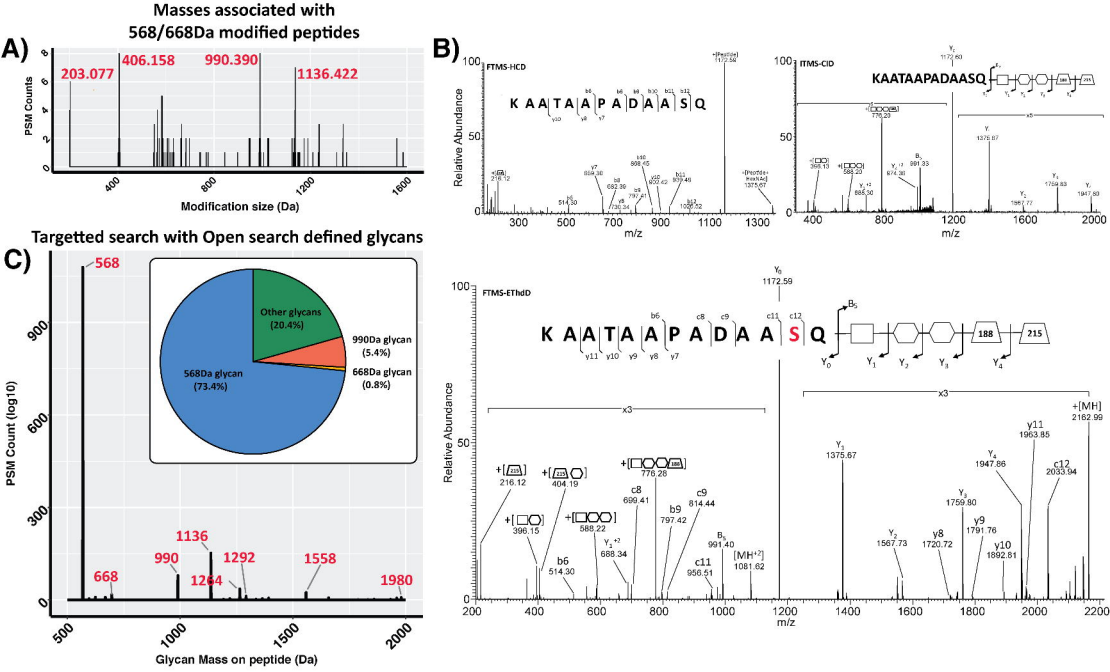
A)
Masses associated with
568/668Da modified peptides
203.077
406.158
990.390
1136.422
PSM Counts
Modification size (Da)
B)
FTMS-HCD
ITMS-CID
FTMS-EThdD
KAATAAPADAASQ
Relative Abundance
m/z
C)
Targetted search with Open search defined glycans
568
990
1136
1264
1292
1558
1980
668
Other glycans
(20.4%)
990Da glycan
(5.4%)
668Da glycan
(0.8%)
568Da glycan
(73.4%)
PSM Count (log10)
Glycan Mass on peptide (Da)